University of Baghdad
College of Engineering
JOURNAL OF ENGINEERING

Journal of Engineering

journal homepage: www.jcoeng.edu.iq

Volume 31 Number 9 September 2025

Performance Evaluation of Perovskite Solar Module of Wide Range Operating Conditions

Omar M. Shaker *, **Adawiya A. Hamzah** , **Emad T. Hashim**

Department of Energy, College of Engineering, University of Baghdad, Baghdad, Iraq

ABSTRACT

Solar energy is considered a sustainable and clean source of power. Even so, solar cells face challenges such as the low efficiency of some systems and the need for large installation areas. Therefore, efforts have been directed toward developing technologies like perovskite solar cells to improve efficiency and reduce the need for large spaces. The experimental work was conducted under outdoor exposure in Baghdad, Al-Jaderia. The readings were taken on selected days, where the atmospheric conditions of clear sky. To study the impacts of temperature variations on solar performance, solar irradiance must be kept constant and vice versa. Therefore, to have a temperature range and for more accuracy, the measurements were done for the tested module with five solar radiation levels: 200, 400, 600, 800, and 1000 W/m^2. The optimum conditions that it have the best performance are achieved when the solar module works at a low ambient temperature. The highest power at solar radiation 1000W/m^2 was 446.2 mW and at module temperature 43 C°, while the minimum corresponding 64 mW at solar radiation 200W/m^2 and module temperature of 43.6 C°. The highest open voltage equals 10.80 V, and at a module temperature of 43 C°, and maximum short current 77 mA at solar irradiance 1000W/m^2 and module temperature 58 C°. The best value of fill factor was achieved 0.661 at solar irradiance 200 W/m^2 and module temperature 43.6 C°. While the best efficiency value 8.9 % at solar radiation 1000 W/m^2, and module temperature 43 C°.

Keywords: Perovskite solar module, Voltage, Current, Power, Solar irradiance.

1. INTRODUCTION

Today, more work has been done in photovoltaic (PV) technology because of the introduction of new generation solar systems **(Kosyachenko et al., 2014; Chatzisideris et al., 2016; Xu et al., 2017)**. Perovskite have the newest photovoltaic technology, because of low price and high efficiency **(Wang et al., 2015; Huang et al., 2015; Kung et al., 2015)**. Perovskite materials are the key to high solar module performance and activity, and many workers try to achieve that **(Haider et al., 2020; Cui et al., 2014; Rahul et al., 2017)**.

*Corresponding author
Peer review under the responsibility of University of Baghdad.
https://doi.org/10.31026/j.eng.2025.09.08
This is an open access article under the CC BY 4 license (http://creativecommons.org/licenses/by/4.0/).
Article received: 15/04/2025
Article revised: 13/06/2025
Article accepted: 25/06/2025
Article published: 01/09/2025

The first Pervoskite building was made by Tsutomu Miyasaka's Tokyo-based company with an efficiency of 2.2% in 2006 **(Kojima et al., 2006; Yusuf et al., 2024)**, and after a few years, they enhanced it to 3.8% **(Kojima et al., 2009; Ren et al., 2021)**. After that, the efficiency jumped to 25.2% in 2019 **(Shao et al., 2024; Szabó et al., 2023; Hossain et al., 2023).** Enhancement of Perovskite material through the use of different materials, like methylammonium lead tri-iodide-based. Unstable manufacturing materials and toxicity may impose limitations in the production line **(Assadi et al., 2018; Cheng et al., 2016; Lekesi et al., 2022; Minemoto et al., 2020)**. A study on PSCs with a Sn–Ge hybrid perovskite composition ($FA_{0.75}MA_{0.25}Sn_{0.95}Ge_{0.05}I_3$) reported a PCE of 4.48%, alongside enhanced air stability resulting from the Ge incorporation **(Ito et al., 2018; Farhadi et al., 2021; Sabbah et al., 2023).** Recently, a perovskite solar cell designed with a dual absorberion layer structure ($MASnI_3/MAPbI_3$) was simulated and investigated, achieving an impressive power conversion efficiency (PCE) of 30.88%. More work has been done on solar panel modeling and maximum power point tracking **(Hashim et al., 2018 a and b; Mohammed et al., 2019)**. Operating solar module temperature is considered a major parameter affecting solar cell performance **(Hashim and Abbood, 2016)**. They also stated that there is a linear proportionality between outlet power and solar module operating temperature**. (Hashim, 2016; Hashim and Abbood, 2016)**. found the four parameter model using different methods: slope method, and explicit simplified method. The accuracy of these methods, as it's compared with the measured data is 5%, 7.9%, and 9.3%, respectively. **(Katee et al., 2021)** made experimental measurements for current, voltage, and power for two kinds of solar modules. These data were used to extract a four-parameter model using two different extraction methods. For monocrystalline solar panels, the percentage errors are 5% and 8% for the iterative method and simplified explicit, while for the corresponding copper indium gallium diselenide, they are 10% and 9%. More work concerned with modeling solar modules is available in these references **(Hashim et al., 2018; Kadia et al., 2022)**. More recent studies have examined key factors influencing the performance of floating photovoltaic systems on major water bodies in Iraq, along with the simulation of a 100 MW solar power unit **(Abdulhadi et al., 2025; Faisal and Hashim, 2025)**.

The present work aims to make performance evaluation of perovskite solar cells with some important operating conditions like solar radiation and operating module temperature (function of ambient temperature).

2. BASIC ELECTRICAL PARAMETERS FOR SOLAR MODULE

2.1 Short Circuit Current

The short circuit current (I_{sc}) refers to the highest current that a solar cell can produce when there is no external load (i.e., when R_L = 0) or when the circuit is shorted. At this point, the voltage across the cell drops to zero **(Katee et al., 2021)**. These current results from the generation and collection of charge carriers produced by light. The magnitude of I_{sc} is primarily determined by the number of incoming photons, the spectral distribution, the surface area of the cell, its optical characteristics, and how efficiently the photogenerated charge carriers are captured. **Fig. 1** illustrates the graphical representation of $I_{sc.}$

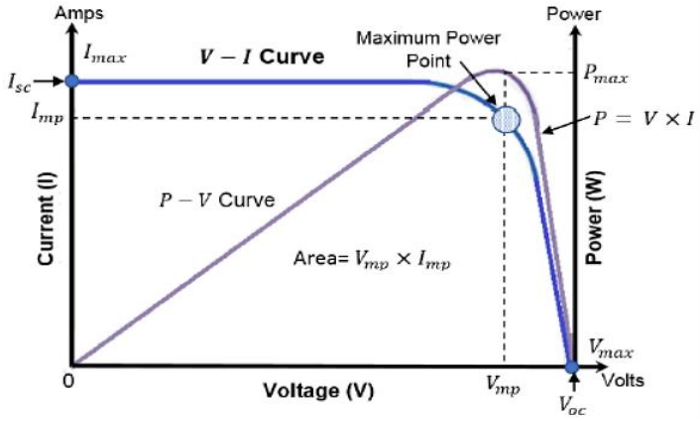

Figure 1. I_{sc} and V_{oc} representing in VI curve **(Katee et al., 2021).**

2.2 Open Circuit Voltage

The maximum voltage extracted from a solar cell when the load of resistance at ($R_L = \infty$) is defined as such open circuit voltage (V_{oc}). Under open-circuit conditions, when no loads are connected to the solar cell, the current becomes zero while the voltage reaches its peak value **(Ullah et al., 2013)**. From the equation of a solar cell, V_{oc} can be derived through setting net current equal to zero, as shown in Eq. (1)**.**

$$V_{oc} = \frac{n\kappa T}{q} ln\left(\frac{I_L}{I_o} + 1\right) at\ I = 0 \quad (1)$$

Based on the equation above, the open-circuit voltage relies on I_0 (saturation current) as well as I_L (light-generated current). I_0 is influenced by the rate of recombination within the solar cells. Thus, V_{oc} serves as an indicator of the level of recombination within a solar cell. The open circuit voltage is illustrated graphically in **Fig. 1.**

2.3 Fill Factor

The fill factor (FF) serves as an indicator of the quality of a photovoltaic cell and is determined by comparing the greatest obtainable power (P_{max}) to the theoretical power (P_t). Where the theoretical output power (P_t) corresponds to the product of the open circuit voltage (V_{oc}) and the short circuit current (I_{sc}) as shown at Eq. (**2**) and (3) **(Khattak et al., 2018)**. Graphically, the fill factor is represented such the ratio between two rectangular areas, as illustrated in **Fig. 1.**

$$FF = \frac{P_{max}}{P_t} \quad (2)$$

$$FF = \frac{V_{max} I_{max}}{V_{oc} I_{sc}} \quad (3)$$

2.4 Maximum Power

The output power of a solar cell, measured in watts, is the result of multiplying the voltage by current and is defined as Eq. (4)**.**

$$P_{out} = V_{out} I_{out} \quad (4)$$

Under both short circuit and open circuit conditions, no power is produced. The output power becomes zero if either the current or the voltage is zero. The system delivers maximum power when both the voltage and current reach their optimal values, as Eq. (5).

$$P_{max} = V_{max} I_{max} \quad (5)$$

The maximum power, expressed in terms of the fill factor, can be calculated using Eq. (3) in Eq. (5) to get Eq. (6).

$$P_{max} = V_{oc} I_{sc} FF \quad (6)$$

2.5 Efficiency

Efficiency (η) represents the relative of effective output power to the total input power, usually quantified in percentage terms, as shown in Eq. (7) and (8).

$$\eta = \frac{P_{out}}{p_{in}} \times 100\% \quad (7)$$

$$\eta = \frac{V \times I}{G \times A} \times 100\% \quad (8)$$

3. METHODOLOGY AND EXPERIMENTAL MEASUREMENTS

A perovskite solar module had been examined, which is from the fourth-generation solar module family. **Table 1** shows the module specifications as given by the manufacturers at reference Standard Test Conditions (STC). The solar cell is calibrated in a fixed procedure supplied by the manufacturer. The Wireless Weather Sensor has 19 measurements: weather, light, and GPS. More details for the Wireless Weather Sensor are available in **Fig. 2**.
Solar module analyzer PROVA 210A is used to test the characteristics (V_{oc}, I_{sc} , V_m , I_m and P_m). PROVA 210A generates the I-V curve by changing an internal resistive load with time from zero to infinity; therefore, for each value of load, there is a value for voltage and current from (0, I_{sc}) to (V_{oc},0). The general specifications of the solar module are given in **Table 2**. A vector for the module output power results from multiplying the I-V vectors. Tracing the maximum point of the power vector gives the value of maximum power, and the respective value of current and voltage locates the point of the highest power. The device has an option to set up the values for both solar radiation and solar area module **Fig. 3**.

Table 1. Perovskite solar module specifications at 25 C° and 1 atm.

Area, cm²	**V_{oc}, V**	**I_{sc}, mA**	**Peak power, mW**	**Peak voltage, V**	**Peak current, mA**	**No. of cells**	**Efficiency %**	**Production data**
56.787	10.999	83.589	703.2	9.35	75.21	1	8.94	2024
Dimensions						Weight, gm		
Length, mm		With, mm		Thickness, mm				
100		100		10		155		

Figure 2. Wireless Weather Sensor with 19 measurements

Table 2 Specifications of solar module analyzer (Prova 210)

Battery type	Rechargeable, 2500mAh (1.2V) * 8	
AC Adaptor	AC 110V or 220V input DC 12V/1~3A output	
Dimension	257(L) * 155(W) * 57(H) mm	
Weight	1160g	
Operation environment	0 °C - 50 °C , 85% RH (relative humidity)	
Temperature coefficient	0.1% of full scale/ °C (< 18 °C or > 28° C)	
Storage environment	-20° C ~ 60 °C , 75% RH	
Accessories	User manual * 1, AC adaptor*1 Optical USB cable*1 Software CD *1, software manual *1 Kelvin clips(6A max) *1 set	
DC voltage measurements		
Range	**Resolution**	**Accuracy**
0-6	0.001V	±1% ±(1% of V_{open}±9 mV)
6-10 V	0.001V	±1% ±(1% of V_{open}±0.09 V)
10-60 V	0.01 V	±1% ±(1% of V_{open}±0.09 V)
DC current measurements		
Range	**Resolution**	**Accuracy**
0.01-6 A	0.1mA	±1% ±(1% of $I_{short\ n}$±0.09 mA)
0.6-61A	0.1mA	±1% ±(1% of $I_{short\ n}$±0.09 mA)
1-6 A	1mA	±1% ±(1% of $I_{short\ n}$±0.09 mA)

4. EXPERIMENTAL WORK PROCEDURE

The present work was done from July 2024 to April 2025. The experimental work was conducted under outdoor exposure in Baghdad- Al-Jaderia. The readings were taken within the time 9:00 am-2:00 pm on selected days (4,11,22,25/9/2024, 1,9,16,23/10/2024, 6,13,18,25/11/2024, 1,11,18,23/12/2024, 8,15,22/1/2025, 27,17/2/2025, 12/3/2025, 6/4/2025, where the atmospheric conditions of clear skies with no clouds, no dusty days, and no rain fell. To study the effects of temperature variations on solar performance, solar irradiance must be kept constant and vice versa. Therefore, to have the temperature range and for higher accuracy, the measurements were done for the tested module with five solar radiation levels: 200, 400, 600, 800, and 1000 W/m^2.

Figure 3. Prova 210A Solar Module Analyzer resp.

The solar module analyzer (Prova 210) needs 10 seconds to make a scan with variable to supply the curves of I-V and P-V characteristic, and this time at outdoor conditions is enough to have a constant solar radiation. The module is cleaned before the tests. The solar module is fixed to the south direction with tilted angle 45^{o} then recording the module back side temperature (using thermocouple) and start the IV scanning process, which is done by the Solar Module Analyzer, then save the data in the computer as illustrated in **Fig. 4**. The diagram of the schematic is shown in **Fig. 5**.

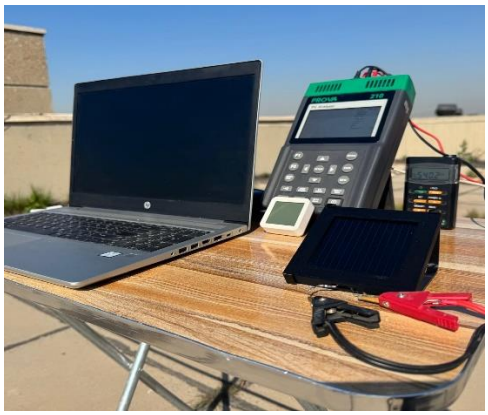

Figure 4. Setup of the experiment

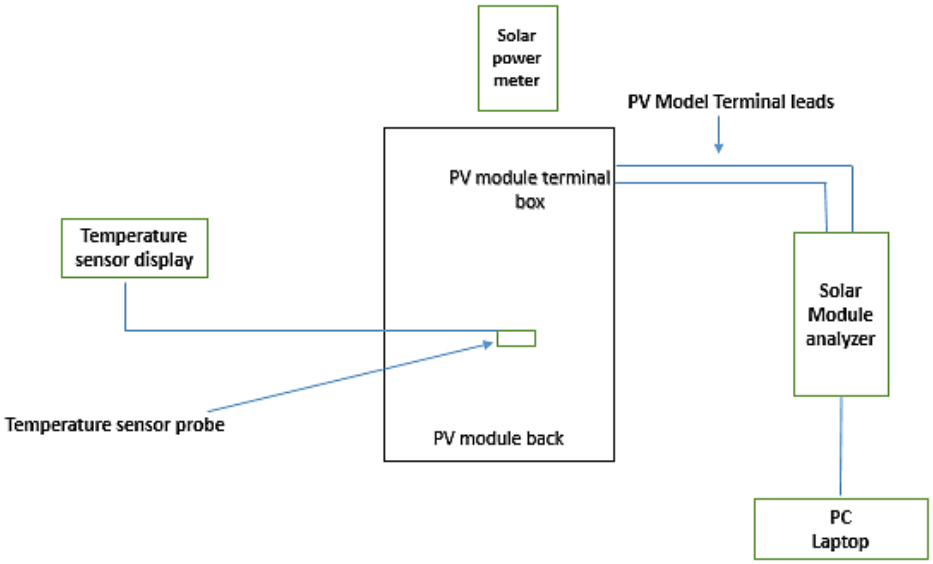

Figure 5. schematic diagram Setup of the experiment

5. RESULTS AND DISCUSSIONS

5.1 Electric Solar Module Parameters

Tables 3-5 show solar Pervoskite photovoltaic solar module parameters T_c(C°), V_{oc}(V), I_{sc}(A), P_{max}(W), V_{max}(V), I_{max}(A), η (%), and FF) with solar module operation temperature for solar irradiance of 200, 400, 600, 800 and 1000 W/m^2 respectively. Tables 3-5 also contain solar module temperature (T_c). The heat generated in the module depends on the amount of solar radiation incident on the module and, conversion efficiency.

The maximum power (P_{max}) at solar radiation intensity 1000W/m^2 is 446.2 mW and at module temperature 43 ^{o}C, while the minimum corresponding one is 64 mW at solar irradiance 200W/m^2 and module temperature of 43.6 C°.The highest open voltage equals to 10.80 V, and at a module temperature of 43 C°, and maximum short current is equal to 77 mA, and at solar irradiance 1000W/m^2 module temperature is 58 C°. The best value of FF achieved is 0.661 at G=200 W/m^2 and T_c=43.6 C°. While the best efficiency value is 8.9 % at G=1000 W/m^2 and T_c=43 C°.

Table 3. Electrical parameters of Perovskite photovoltaic solar module at different solar radiation and ambient temperature of 25 C°

T_c C°	G W/m^2	V_{oc} V	I_{sc} mA	V_m V	I_m mA	P_m mW	FF	η %
28.6	200	9.444	14	5.415	13	69.31	0.524	6.9
32.2	400	10.01	26	5.647	22	124.7	0.486	6.2
35.8	600	10.36	41	5.800	35	200.1	0.466	6.6
39.4	800	10.55	58	8.328	35	292.3	0.478	7.3
43	1000	10.80	71	7.761	58	446.2	0.583	8.9

Table 4. Electrical parameters of Perovskite photovoltaic solar module at different solar radiation and ambient temperature of 30 C°

T_c C°	G W/m^2	V_{oc}, V	I_{sc} mA	V_m V	I_m mA	P_m mW	FF	η %
33.6	200	9.228	18	5.392	16	83.6	0.508	8.3
37.2	400	9.758	33	5.399	29	156.5	0.493	7.8
40.8	600	9.986	48	7.927	31	247.3	0.511	8.2
44.4	800	10.13	61	7.666	42	323.5	0.524	8.1
48	1000	10.54	71	7.588	56	427.9	0.575	8.6

Table 5. Electrical parameters of Perovskite photovoltaic solar module at different solar radiation and ambient temperature of 40 °C.

T_c C°	G W/m^2	V_{oc} V	I_{sc} mA	V_m V	I_m mA	P_m mW	FF	η %
43.6	200	8.038	12	5.802	11	64	0.661	5.6
47.2	400	8.746	32	6.407	25	162	0.572	7.1
50.8	600	8.85	30	6.401	21	136	0.506	3.9
54.4	800	9.342	59	6.579	38	253	0.453	5.5
58	1000	9.64	77	6.494	50	324	0.437	5.7

Figs. 6 to 11 shows the usual I-V and P-V curves at the selected solar radiations, 200,400, 600,800, and 1000 W/m^2 and at varous ambient temperatures: 25, 30, and 40 C°. The characteristic curves (voltage-current and voltage–power) are examined with solar module factors. The different I-V and P-V curves are investigated by varying solar cell parameters. For ambient temperature 25 C°, 30 C°, and 40 C°, irradiation modifications are rendered (200W/m^2, 400W/m^2, 600W/m^2, 800 W/m^2,1000W/m^2)

5.2 Characteristic Voltage-current and Voltage-power Curves of Solar Module

Figs. 6-11 summarizes the characteristic curves for the mentioned conditions. More power will be attained by more solar insolation incident and which leads to high current. The photo current generated by the incident light remains largely stable, with only a slight increase observed as the voltage varies. Voltage and power are reduced by solar module temperature increase.

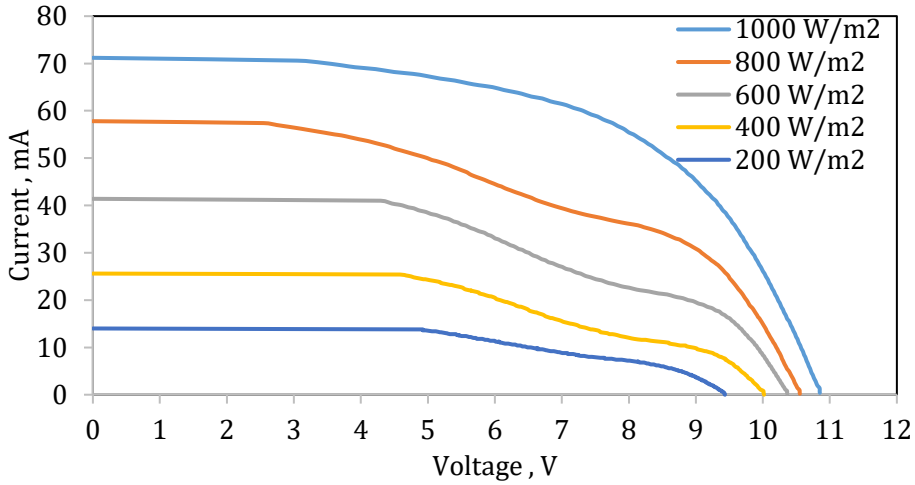

Figure 6. Voltage-current characteristic curve of perovskite solar module at different solar insolation and ambient temperature of 25 C°

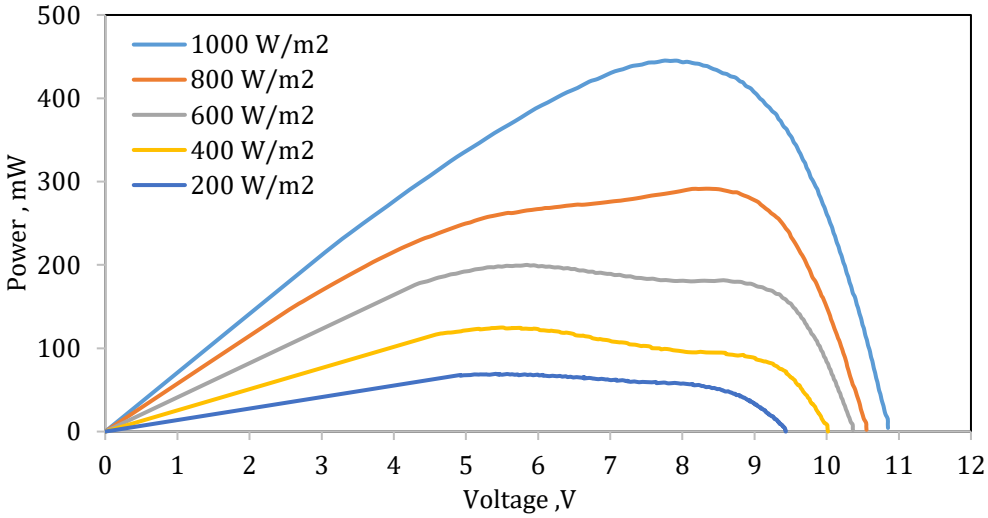

Figure 7. Voltage-power characteristic curve of perovskite solar module at different solar insolation and ambient temperature of 25 C°.

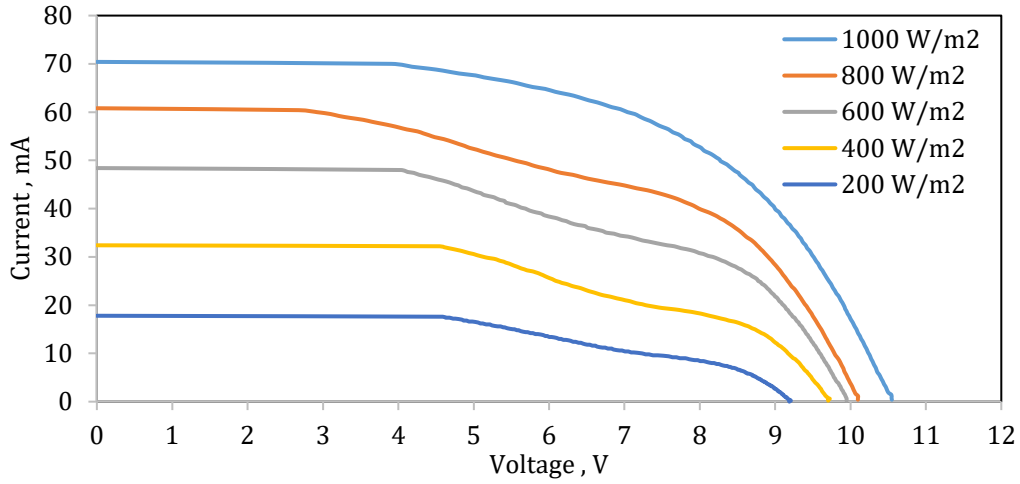

Figure 8. Voltage-current characteristic curve of perovskite solar module at different solar insolation and ambient temperature of 30 C°

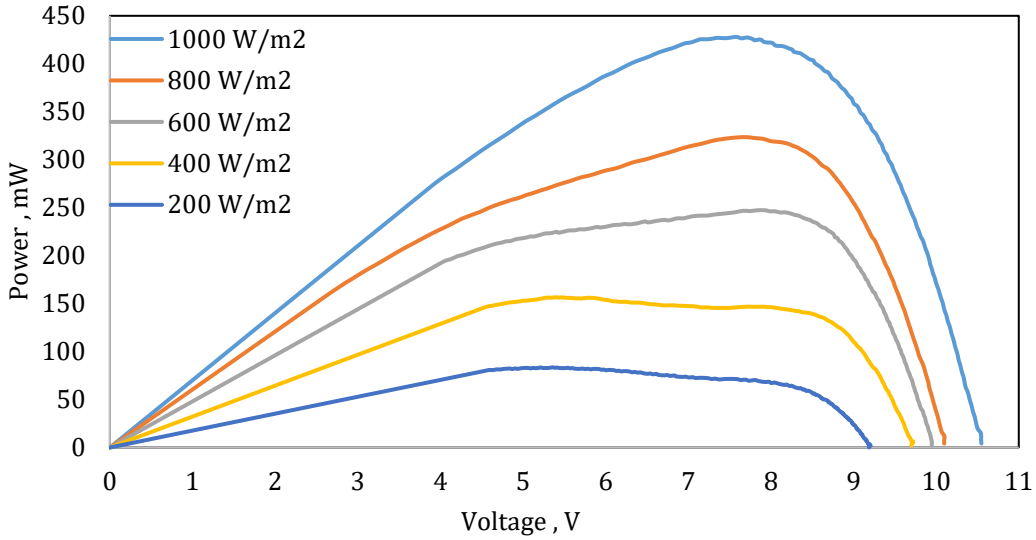

Figure 9. Voltage-power characteristic curve of perovskite solar module at different solar insolation and ambient temperature of 30 C°

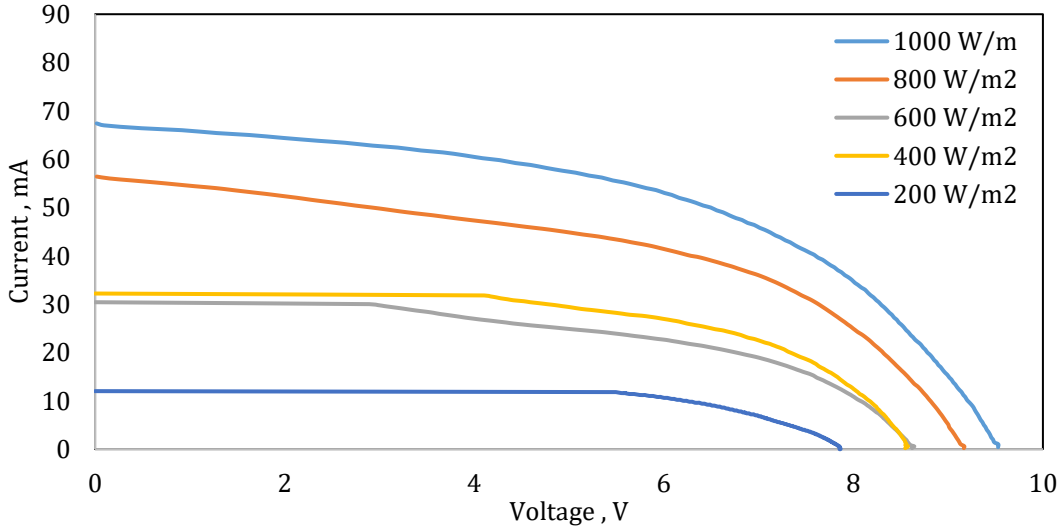

Figure 10. Voltage-current characteristic curve of perovskite solar module at different solar insolation and ambient temperature of 40 C°

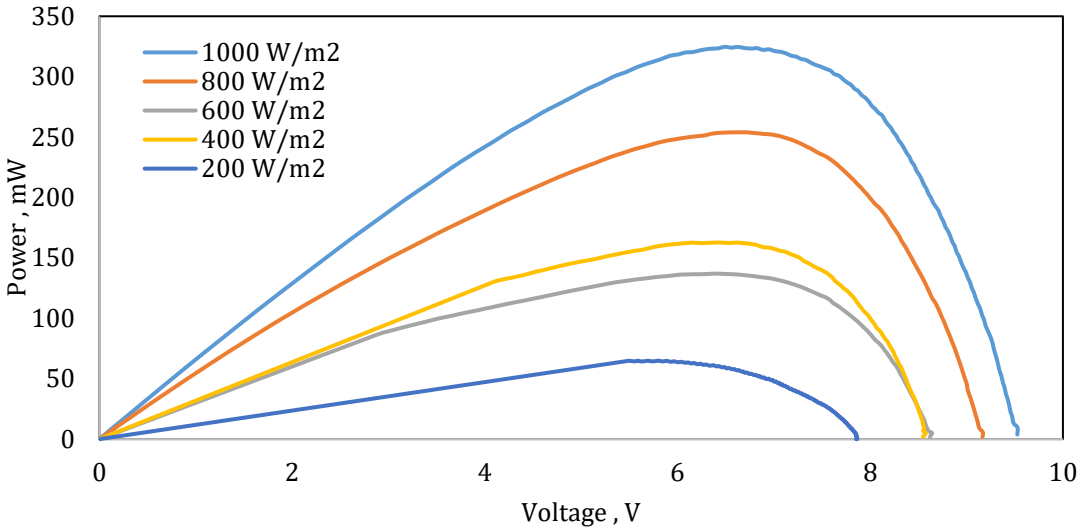

Figure 11. Voltage-power characteristic curve of perovskite solar module at different solar insolation and ambient temperature of 40 C°

5.3 Solar Module Operating Temperature Effect on I_{sc}, V_{oc}, and P_{max}

The temperature sensitivity of PV modules is a critical aspect of their electrical output performance. During operation, a significant portion of solar irradiance is transformed into useful electricity, typically around 20%, while the remainder is dissipated as heat. This heat generation increases the module operating temperature, which in turn affects the module's electrical parameters, particularly the open-circuit voltage (V_{oc}). An elevated operating temperature can have detrimental effects on the performance of PV modules. Higher temperatures generally reduce the V_{oc}, which is an essential parameter for optimizing the system's power output. A lower V_{oc} means that the module needs to apply more voltage to initiate electricity generation, leading to a decrease in overall power output. This reduction in power output can strongly influence the efficiency and profitability of solar energy systems. Increasing the operating solar module led to an increase in reverse saturation current of photvoltic module (recombination of photons) and this will lead to a power drop and decrease in module efficiency and performance. In fact, the optimum conditions for optimum performance of a solar module when it is operated at low temperature. Moreover, the temperature variation also affects other electrical parameters of the Pervoskite solar module, like fill factor (FF) and short circuit current (I_{sc}) . These parameters are also critical for enhancing the performance of the solar system. As temperatures rise, the I_{sc} and FF typically decrease, further contributing to the reduction in power output. Understanding the temperature sensitivity of PV modules and the associated electrical parameters is crucial for designing, installing, and maintaining solar energy systems. By accounting for temperature fluctuations and their impact on module performance, researchers and system designers can develop strategies to mitigate these effects and ensure that solar energy systems operate efficiently and effectively over their entire operating temperature range.

To analyze the data, a scatter plot was used between I_{sc} and V_{oc} for different solar irradiances:200, 400, 600, 800, and 1000 W/m^2, and the corresponding module operating temperatures (available in **Figs. 12 and 13**). **Fig. 12** shows a slight increase in I_{sc} values and a decrease in V_{oc} values represented in **Fig.13**.

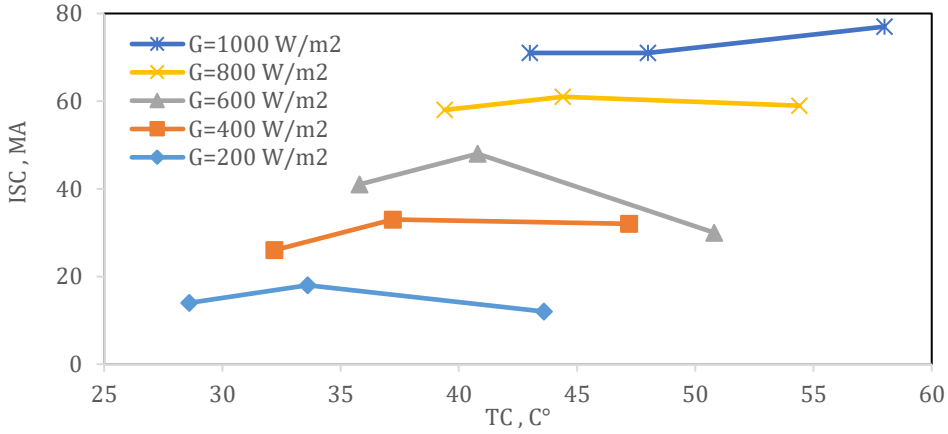

Figure 12. Variation of short circuit current (I_{sc}) with operating solar module temperature (T_c) at different solar radiations (G).

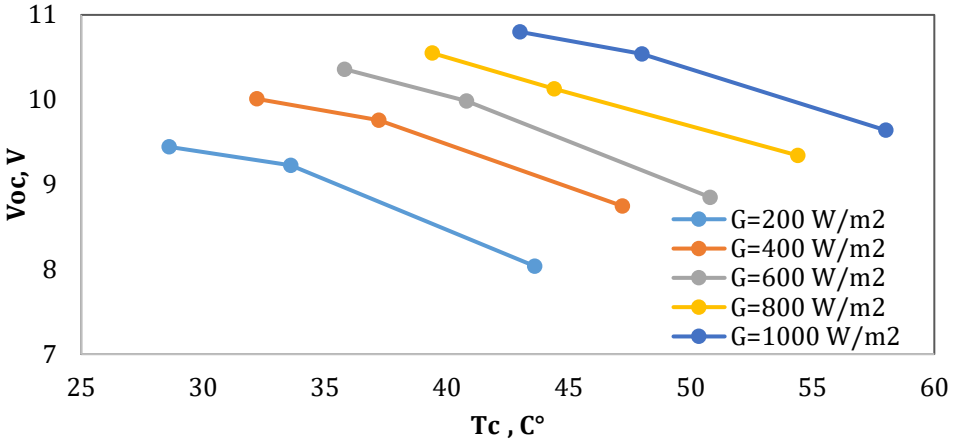

Figure 13. Variation of open circuit voltage (V_{oc}) with operating solar module (T_c) temperature at different solar radiations (G)

Fig.14 shows the variation of maximum power (P_{max}) voltage with operating solar module (T_c) temperature at different solar radiations (G), which summarizes an increase of solar module power output with increasing solar radiation despite module temperature change. The highest value of power at solar radiation intensity 1000W/m^2 was 456.6 mW, and the minimum corresponding one is 64 mW at solar irradiance 200W/m^2.

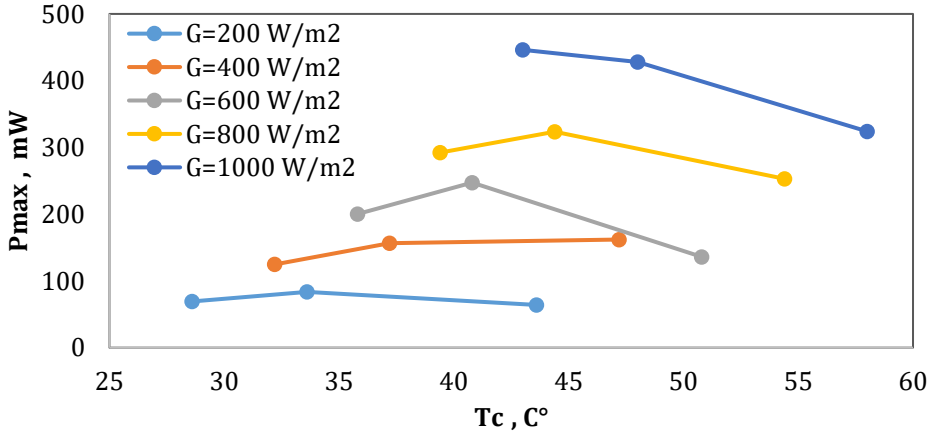

Figure 14. Variation of maximum power (P_{max}) with operating solar module (T_c) temperature at different solar radiations (G)

5. CONCLUSIONS

Higher temperatures generally reduce the V_{oc}, which is an essential parameter for optimizing the system's power output. The temperature variation also affects other electrical parameters of the Pervoskite solar module, like short circuit current (I_{sc}) and fill factor (FF). A reduction in power output can significantly impact the efficiency and profitability of solar energy systems. This reduction in the power of solar modules is a function of the decrease in solar irradiance values. The maximum value of power at solar radiation intensity 1000W/m^2 was 456.6 mW, and the minimum corresponding one is 64 mW at solar irradiance 200W/m^2. Finally, one can conclude that optimum module performance is attained with the lowest module operating temperature. For future work, more work needs to be done on environmental conditions on pervoskite solar module, like; humidity, dust, shadow, soiling, and wind speed.

NOMENCLATURE

Symbol	Description	Symbol	Description
G	Irradiance, W/m2	FF	Fill factor
I_{sc}	Short circuit current, A	P_{max}	maximum power, W
I_{max}	Maximum current, A	V_{max}	maximum voltage, V
T_a	Ambient temperature, **C°**	V_{oc}	Open circuit voltage, V
T_c	Operating solar module temperature, **C°**	η	Solar module efficiency, %
k	Constant of Boltzmann (1.3805×10^{-23} J/K)	q	Charge of Electron (1.602×10^{-19} C)

Credit Authorship Contribution Statement

Omar Mohammed Shaker: Experimental work, Writing, Validation, Methodology. Emad Talib Hashim: Review and editing, Validation, Proofreading. Adawiya Ali Hamzah: Review and editing, Validation, Proofreading.

Declaration of Competing Interest

The authors declare that they have no known competing financial interests or personal relationships that could have appeared to influence the work reported in this paper.

REFERENCES

Abdulhadi, Z.A., Hashim, E.T., and Tolephih, M.H., 2025. Investigation of some key factors impacting floating photovoltaic solar system performance on major Iraq water bodies. *Journal of Engineering*, 31(3), pp. 63-80. https://doi.org/10.31026/j.eng.2025.03.04

Assadi, M.K., Bakhoda, S., Saidur, R,. and Hanaei, H., 2018. Recent progress in perovskite solar cells. *Renewable and Sustainable Energy Reviews*, 81, pp. 2812-2822. https://doi.org/10.1016/j.rser.2017.06.088

Chatzisideris, M.D., Espinosa, N., Laurent, A., and Krebs, F.C., 2016. Ecodesign perspectives of thin-film photovoltaic technologies: A review of life cycle assessment studies. *Solar Energy Materials and Solar Cells*, 156, pp. 2-10. https://doi.org/10.1016/j.solmat.2016.05.048

Cheng, P., and Zhan, X., 2016. Stability of organic solar cells: Challenges and strategies. *Chemical Society Reviews*, 45(9), pp. 2544-2582. https://doi.org/10.1039/C5CS00593K

Cui, J., Meng, F., Zhang, H., Cao, K., Yuan, H., Cheng, Y., Huang, F., and Wang, M., 2014. CH3NH3PbI3-based planar solar cells with magnetron-sputtered nickel oxide. *ACS applied materials and interfaces*, 6(24), pp. 22862-22870. https://doi.org/10.1021/am507108u

Faisal, S.S., and Hashim, E.T., 2025. An approach to solar photovoltaic systems simulation utilizing builder block: a case study of a 100 MW system. *Journal of Engineering*, 31(1), pp. 98-119. https://doi.org/10.31026/j.eng.2025.01.06

Farhadi, B., Ciprian, M., Zabihi, F., and Liu, A., 2021. Influence of contact electrode and light power on the efficiency of tandem perovskite solar cell: Numerical simulation. *Solar Energy*, 226, pp. 161-172. https://doi.org/10.1016/j.solener.2021.08.043

Hahsim, E.T., 2016. Determination of mono-crystalline Silicon photovoltaic module parameters using three different methods. *Journal of Engineering*, 22(7), pp. 92-107. https://doi.org/10.31026/j.eng.2016.07.06

Hashim, E.T., and Hussien, S.A.M., 2018. Synchronous buck converter with perturb and observe maximum power point tracking implemented on a low-cost arduino-microcontroller. *Journal of Engineering*, 24(2), pp. 16-33. https://doi.org/10.31026/j.eng.2018.02.02.

Hashim, E.T., and Talib, Z. R. 2018 a. Study of the performance of the five-parameter model for a monocrystalline silicon photovoltaic module using reference data .*FME Transactions*, 46, pp. 585-594. https://doi.org/10.5937/fmet1804585T

Hashim, E. T., and Talib, Z. R., 2018 b. Modeling and simulation of solar module performance using the parameters model by using Matlab in Baghdad city. *Journal of Engineering,* 24(10), pp. 15-31. https://doi.org/10.31026/j.eng.2018.10.02.

Hashim, E.T., and Abbood, A.A., 2016. Temperature effect on power drop of different photovoltaic modules. *Journal of Engineering*, 22(5), pp. 129-143. https://doi.org/10.31026/j.eng.2016.05.09

Haider, M., and Yang, J.L., 2020. Efficient and stable perovskite–silicon two-terminal tandem solar cells. *Rare Metals*, 39(7), pp. 745-747. https://doi.org/10.1007/s12598-020-01430-4

Hossain, M.K., Toki, G.I., Samajdar, D.P., Mushtaq, M., Rubel, M.H.K., Pandey, R., Madan, J., Mohammed, M.K., Islam, M.R., Rahman, M.F., and Bencherif, H., 2023. Deep insights into the coupled optoelectronic and photovoltaic analysis of lead-free CsSnI3 perovskite-based solar cell using DFT calculations and SCAPS-1D simulations. *ACS Omega*, 8(25), pp. 22466-22485.

Huang, Z., Xu, W., and Yu, K., 2015. Bidirectional LSTM-CRF models for sequence tagging. arXiv preprint arXiv:1508.01991. https://doi.org/10.48550/arXiv.1508.01991

Ito, N., Kamarudin, M.A., Hirotani, D., Zhang, Y., Shen, Q., Ogomi, Y., Iikubo, S., Minemoto, T., Yoshino, K., and Hayase, S., 2018. Mixed Sn–Ge perovskite for enhanced perovskite solar cell performance in air. *The Journal Of Physical Chemistry Letters*, 9(7), pp. 1682-1688. https://doi.org/10.1021/acs.jpclett.8b00275

Kadia, N.J., Hashim E. T., and Abdullah, I. B., 2022. Performance of different photovoltaic technologies for amorphous Silicon (A-Si) and Copper Indium Gallium Di-Selenide (CIGS) Photovoltaic Modules. *Journal of Engineering and Sustainable Development*, *26*(1), pp. 95-105.

Katee, N.S., Abdullah, O.I., and Hashim, E.T. 2021. Extracting four solar model electrical parameters of mono-crystalline silicon (mc-Si) and thin film (CIGS) solar modules using different methods. *Journal of Engineering*, 27(4), pp. 16-32. https://doi.org/10.31026/j.eng.2021.04.02

Khattak, Y.H., Baig, F., Ullah, S., Mari, B., Beg, S. and Ullah, H., 2018. Numerical modeling baseline for high efficiency (Cu2FeSnS4) CFTS based thin film kesterite solar cell. *Optik*, *164*, pp. 547-555.

Kojima, A., Teshima, K., Miyasaka, T., and Shirai, Y., 2006, June. Novel photoelectrochemical cell with mesoscopic electrodes sensitized by lead-halide compounds (2). *In ECS Meeting Abstracts*, 7, P. 397. IOP Publishing.

Kojima, A., Teshima, K., Shirai, Y., and Miyasaka, T. 2009. Organometal halide perovskites as visible-light sensitizers for photovoltaic cells. *Journal of the American Chemical Society*, *131*(17), pp. 6050-6051. https://doi.org/10.1021/ja809598r

Kosyachenko, L.A., Mathew, X., Paulson, P.D., Lytvynenko, V.Y., and Maslyanchuk, O.L., 2014. Optical and recombination losses in thin-film Cu (In, Ga) Se2 solar cells. *Solar Energy Materials And Solar Cells*, 130, pp. 291-302. https://doi.org/10.1016/j.solmat.2014.07.019

Kung, J.T., Kesner, B., An, J.Y., Ahn, J.Y., Cifuentes-Rojas, C., Colognori, D., Jeon, Y., Szanto, A., del Rosario, B.C., Pinter, S.F., and Erwin, J.A., 2015. Locus-specific targeting to the X chromosome revealed by the RNA interactome of CTCF. *Molecular Cell*, 57(2), pp. 361-375.

Lekesi, L.P., Koao, L.F., Motloung, S.V., Motaung, T.E., and Malevu, T., 2022. Developments on perovskite solar cells (PSCs): A critical review. *Applied Sciences*, 12(2), P. 672. https://doi.org/10.3390/app12020672

Minemoto, T., Kawano, Y., Nishimura, T., Shen, Q., Yoshino, K., Iikubo, S., Hayase, S., and Chantana, J., 2020. Theoretical analysis of band alignment at back junction in Sn–Ge perovskite solar cells with inverted pin structure. *Solar Energy Materials and Solar Cells*, 206, P. 110268. https://doi.org/10.1016/j.solmat.2019.110268

Mohammed, S.A., and Hashim, E.T., 2019. Designing a maximum power point tracking system for a monocrystalline silicon solar module using the arduino microcontroller and synchronous buck converter. *FME Transactions*, 47, pp. 524-533. http://doi.org/10.5937/fmet1903524M

Rahul, Abhishek, K., Datta, S., Biswal, B.B., and Mahapatra, S.S. 2017. Machining performance optimization for electro-discharge machining of Inconel 601, 625, 718 and 825: an integrated optimization route combining satisfaction function, fuzzy inference system, and Taguchi approach. *Journal of the Brazilian Society of Mechanical Sciences and Engineering*, *39*, pp. 3499-3527. https://doi.org/10.1007/s40430-016-0659-7

Ren, G., Han, W., Deng, Y., Wu, W., Li, Z., Guo, J., and Guo, W. 2021. Strategies of modifying spiro-OMeTAD materials for perovskite solar cells: a review. *Journal of Materials Chemistry A*, *9*(8), pp. 4589-4625.

Sabbah, H., and Baki, Z. A. 2023. Device simulation of highly stable and 29% efficient FA 0.75 MA 0.25 Sn 0.95 Ge 0.05 I 3-based perovskite solar cell. *Nanomaterials*, *13*(9), P. 1537. http://doi.org/10.3390/nano13091537

Shao, Y., Zheng, D., Liu, L., Liu, J., Du, M., Peng, L., and Liu, S. 2024. Innovations in interconnecting layers for perovskite-based tandem solar cells. *ACS Energy Letters*, *9*(10), pp. 4892-4921. https://doi.org/10.7498/aps.73.20241187

Szabó, G., Park, N.G., De Angelis, F., and Kamat, P. V. 2023. Are perovskite solar cells reaching the efficiency and voltage limits?. *ACS Energy Letters*, *8*(9), pp. 3829-3831.

Ullah H., Marí, B., Cui, H.N., 2013, Investigation on the effect of gallium on the efficiency of CIGS solar cells through dedicated software, *Appl. Mech. Mater*. 448–453, pp. 1497–1501. http://doi.org/10.4028/www.scientific.net/AMM.448-453.1497

Wang, W., Arora, R., Livescu, K., and Bilmes, J. 2015, June. On deep multi-view representation learning. In *International Conference on machine learning* (pp. 1083-1092). PMLR.

Xu, X., Zhao, Y., Sima, J., Zhao, L., Mašek, O., and Cao, X. 2017. Indispensable role of biochar-inherent mineral constituents in its environmental applications: A review. *Bioresource Technology*, *241*, pp. 887-899. https://doi.org/10.1016/j.biortech.2017.06.023

Yusuf, A.S., Ramalan, A.M., Abubakar, A.A., and Mohammed, I.K. 2024. Effect of electron transport layers, interface defect density, and working temperature on perovskite solar cells using SCAPS 1-D Software. *East European Journal of Physics*, (1), pp. 332-341. https://doi.org/10.26565/2312-4334-2024-1-31

تقييم أداء وحدة الخلايا الشمسية البيروفسكايتية تحت نطاق واسع من ظروف التشغيل

عمر محمد شاكر*، عدوية علي حمزة، عماد طالب هاشم

قسم الطاقة ، كلية الهندسة ، جامعة بغداد ، بغداد ، العراق

الخلاصة

تعتبر الطاقة الشمسية مصدرا مستداما و نظيفا للطاقة, ومع ذلك تواجه الخلايا الشمسية تحديات مثل انخفاض كفاءة بعض الأنظمة و حاجتها لمساحات واسعة وقد تم التوجه الى تطوير تقنيات مثل خلايا البيروفسكايت الشمسية لتحسين الكفاءة و تقليل الحاجة للمساحات الكبيرة. تم إجراء العمل التجريبي تحت ظروف التعرض الخارجي في بغداد – الجادرية. تم أخذ القراءات في أيام محددة، حيث كانت الظروف الجوية عبارة عن سماء صافية دون غيوم. ولدراسة تأثير تغيرات درجة الحرارة على أداء الطاقة الشمسية، يجب الحفاظ على ثبات الإشعاع الشمسي، والعكس صحيح وللحصول على مدى واسع من درجات الحرارة وزيادة الدقة، تم إجراء القياسات للوحدة الشمسية المختبرة عند خمسة مستويات من الإشعاع الشمسي: 200، 400، 600، 800 و1000 واط/م². أعلى قدرة تم تسجيلها كانت 446.2 ميلي واط عند شدة إشعاع شمسي مقدارها 1000 واط/م² ودرجة حرارة الخلية بلغت 43 درجة مئوية، في حين أن أقل قيمة للقدرة كانت 64 ميلي واط عند إشعاع شمسي مقداره 200 واط/م² ودرجة حرارة الخلية 43.6 درجة مئوية.أقصى جهد في حالة الدائرة المفتوحة بلغ 10.80 فولت عند درجة حرارة الخلية 43 درجة مئوية عند إشعاع شمسي 1000 واط/م²، وأقصى تيار في حالة القصر 77 ميلي أمبير عند إشعاع شمسي مقداره 1000 واط/م² ودرجة حرارة الخلية 58 درجة مئوية. تم تحقيق أفضل قيمة لعامل الامتلاء وبلغت 0.661 عند شدة إشعاع شمسي 200 واط/م² ودرجة حرارة للوحدة 43.6 في حين سُجلت أعلى كفاءة تحويل للطاقة بنسبة 8.9% عند شدة إشعاع 1000 واط/م² ودرجة حرارة 43 درجة مئوية.

الكلمات المفتاحية: وحدة شمسية من البيروفسكايت ، الإشعاع الشمسي ، الجهد الكهربائي ، التيار الكهربائي ، القدرة.